

Analysis of photoemission in amorphous SiO_x and SiN_x alloys in terms of a charge-transfer model

S. Hasegawa, L. He, T. Inokuma, and Y. Kurata

Department of Electronics, Faculty of Technology, Kanazawa University, Kanazawa 920, Japan

(Received 5 June 1992)

Shifts of the Si 2*p*, O 1*s*, and N 1*s* core-level spectra with the O or N content *x* for amorphous (*a*-) SiO_x and SiN_x films were examined by means of the effective-charge-analysis (ECA) model, in which the averaged partial charge $P_M(x)$ ($M = \text{Si}, \text{O}, \text{or N}$) on a given atom is expressed as a function of *x*, by using Sanderson's electronegativity results and the random-bonding model (RBM). The effective Si 2*p* binding energy $E_B(\text{Si } 2p)$ was found to be linearly related to $P_{\text{Si}}(x)$ per single bond, $E_B(\text{Si } 2p) = 10.2P_{\text{Si}}(x) + 99.3$, independent of sample type. This equation predicts that addition of a unit of positive charge onto a Si atom shifts the Si 2*p* core level downward by 2.55 eV. Furthermore, the ECA model showed that spacing of the Si 2*p* lines due to five $\text{Si}(\text{Si}_{4-n}\text{M}_n)$ ($M = \text{O or N}$) bonding units based on the RBM decreases with increasing *n*, in contrast to an assumption made by many workers. The evaluated negative partial charge, $P_{\text{O}}(x)$ or $P_{\text{N}}(x)$, on an O or N atom is found to decrease with increasing *x*, and the observed $E_B(\text{O } 1s)$ and $E_B(\text{N } 1s)$ are also linearly related to $P_{\text{O}}(x)$ and $P_{\text{N}}(x)$, respectively. Both the O 1*s* and N 1*s* core levels were shown to shift downward by around 1.2 eV as a unit negative charge is subtracted from the O and N atom.

I. INTRODUCTION

Silicon oxide and silicon nitride films are widely used in a variety of electronic devices as the insulator in metal-insulator-semiconductor devices and metal-nitride-oxide-semiconductor memory devices,¹⁻⁴ as passivation layers,⁵ and as heterojunction superlattices.² Amorphous (*a*-) SiO_x and SiN_x films can be prepared over a wide range of O or N content *x* by preparation methods, such as plasma-enhanced chemical vapor deposition (PECVD),^{5,7-11} sputtering,¹²⁻¹⁴ and ion implantation.^{15,16} Since the electronic properties of these layers that depend on *x* affect the device performance, their chemical bonding and electronic structure have been investigated by means of photoemission^{10,12-16} and vibrational absorption^{7,11,17,18} techniques. According to the picture of local bonding at Si sites in SiO_2 and Si_3N_4 , a Si atom with four O or N nearest neighbors takes a tetrahedral structure, an O atom is bonded to two Si atoms, and a N atom is in the center of an equilateral triangle of three Si atoms.^{19,20} In the *a*- SiO_x and *a*- SiN_x films, four Si nearest neighbors in a Si-centered tetrahedron are replaced by O or N atoms at higher content *x*, but the bonding structure at the O and N sites is essentially preserved in SiO_2 and Si_3N_4 , respectively.¹¹⁻¹⁴ Zero or fewer O-O and N-N bonds are interpreted as indicating preferential formation of heteronuclear bonds (chemical ordering).

X-ray-induced photoelectron spectroscopy (XPS) provides information about the microstructure in SiO_x and SiN_x .^{10,12-16} Kärcher, Ley, and Johnson¹² have reported that a successive increase in the binding energy E_B of the Si 2*p* core level in *a*- SiN_x films, with an increase in the N content *x*, could be interpreted in terms of a superposition of five $\text{Si}(\text{Si}_{4-n}\text{N}_n)$ ($n = 0, 1, \dots, 4$) bonding configurations using a curve-fitting method. These au-

thors also found a shift of the N 1*s* XPS line in the same direction as that of the Si 2*p* line, and suggested that it arose from a shift of the Fermi level with *x*. Ingo *et al.*¹⁴ and Bell and Ley¹³ have analyzed, for *a*- SiN_x and *a*- SiO_x films, respectively, the Si 2*p* line on the basis of the random-bonding model (RBM), in which there is a statistical distribution of the above five $\text{Si}(\text{Si}_{4-n}\text{N}_n)$ or $\text{Si}(\text{Si}_{4-n}\text{O}_n)$ configurations. Decomposition of the XPS spectra into five components using a curve-fitting method, however, cannot be performed uniquely because of the uncertainty in the linewidth and the separation energy for the XPS line due to each component.¹² In order to avoid the uncertainty in a fitting method, Hasegawa, Tsukao, and Zalm¹⁰ and Hasegawa and Zalm,¹⁶ for *a*- SiN_x films, proposed an explanation in terms of a weighted-average coordination number n_{av} at a Si site in SiN_n , in which E_B at the center of gravity of the observed Si 2*p* line is predicted to be proportional to n_{av} , which is given by $3x$ under the RBM. In this model, however, it is also assumed that the peak energy for each component of the above five configurations is equally spaced. These authors¹⁰ also suggested that a shift of the N 1*s* line with *x* is connected with the increased number of next-nearest and further far-neighbor N atoms, which is a so-called induction effect.

Such a chemical shift of the Si 2*p* core level has been understood to be brought about by the charge transfer from Si to more electronegative atoms such as O, N, or C.^{10,12-14,16,21} Katayama, Usami, and Shimada²¹ showed that the Si 2*p* binding energy for Si, SiC, Si_3N_4 and SiO_2 is proportional to the partial charge on the Si atom, evaluated from the electronegativity difference of atoms using the relation given by Pauling.²² However, this method can be applied only to binary compounds with a stoichiometric composition. In the case of Si-related compounds, including H atoms, such a charge transfer

between atoms also leads to a shift of the SiH vibrational absorption.^{7,17} Lucovsky¹⁷ evaluated the electronegativity sum (ENS) of the constituent atomic species bonded to SiH, SiH₂, or SiH₃ using the electronegativities of atoms defined by Sanderson,²³ and has shown that the peak wave number of the SiH absorption is proportional to ENS. Lucovsky's model has also been applied to analyses of the SiH absorption for *a*-SiN_x:H films by using the RBM.⁷ Although the Lucovsky's model will be a useful technique for analyzing shifts of the vibrational spectra, information about the partial charge on a given atom, which dominates the XPS spectrum, cannot be obtained. Furthermore, charge neutrality in a given atomic species cannot be separately examined.

In the present work, we investigate the XPS spectra from the Si 2*p* and O 1*s* core levels in PECVD *a*-SiO_x films. On the basis of the RBM, the charge transfer within a minimum cluster (bonding unit) originating in each of five Si(Si_{4-n}O_n) bonding configurations is examined using the calculation method of partial charge introduced by Sanderson.²⁴ In Sec. II we present a calculation method of partial charge on an atom with use of the RBM. In Sec. III we describe the experimental details of the sample deposition and XPS measurements. In Sec. IV, XPS for *a*-SiO_x films in the present work are investigated as a function of the O content *x*. These results and other published results for *a*-SiN_x films^{10,12,16} are correlated with a change of the partial charge on Si, O, and N atoms as a function of *x*. In Sec. V we summarize these results.

II. CHARGE TRANSFER

A. Partial charge

Using Sanderson's model,²⁴ we will discuss the ionicity of a molecule $A_n B_m$, where *n* and *m* are the number of *A* and *B* atoms, respectively. We assume that charge neutrality holds within each molecule, and that the *A* and *B* atoms in the molecule occupy equivalent bonding sites. Then, from Sanderson's model,²⁴ the partial charge P_A on the *A* atom is given by

$$P_A = (S_{AB} - S_A) / (2.08 S_A^{1/2}), \quad (1)$$

where

$$S_{AB} = (S_A^n S_B^m)^{1/(n+m)}. \quad (2)$$

Here, S_A and S_B , respectively, are the electronegativities

of the *A* and *B* atoms as defined by Sanderson,²⁴ and S_{AB} is the effective electronegativity of the molecule. When we consider the case in which part of valence electrons on an *A* atom with the coordination number of f_c are transferred to more electronegative *B* atoms, the value of P_A means that this part (the ratio of P_A) is equally distributed among all *B* atoms within the molecule. Therefore, charge neutrality also implies $nP_A + mP_B = 0$. Furthermore, the effective positive and negative charges on an *A* and a *B* atom are given by $f_c P_A$ and $f_c P_B$, respectively. Under this condition, P_A can also be seen as the ionicity of the *A* atom per single *A*-*B* bond. One method of checking the validity of Eq. (1) is confirmation of the above charge-neutrality condition. From Eq. (1), this condition is found to be satisfied except for the case where the difference between *n* and *m* is too large. Since this method affords a convenient way of obtaining the ionicity for various bonding units, the ionicity for similar compounds, such as SiO and SiO₂, can be distinguished. For amorphous materials such as *a*-SiO_x and *a*-SiN_x films, if their structure can be seen as a mixture of various bonding units holding charge-neutrality conditions, Eq. (1) will be also applicable to these films. The random-bonding model, which will be described in Sec. II B, will make it possible to decompose the bonding structure into some bonding units.

B. Random-bonding model

In the case of *a*-SiO_x and *a*-SiN_x films, the Si atoms are essentially randomly bonded to O or N atoms.^{7,10-14} The bonding structure under the RBM with chemical ordering are composed of five basic Si(Si_{4-n}O_n) or Si(Si_{4-n}N_n) bonding configurations, and the O and N atoms are bonded to two Si and three Si atoms, respectively. The probability $f_n(x)$ for generating each configuration for a given *x* is shown in Table I. Here, the values of *p* in $f_n(x)$ are $p = 0.5$ for *a*-SiO_x and $p = 0.75$ for *a*-SiN_x. Figure 1 shows $f_n(x)$ as a function of *x* for SiO_x and SiN_x systems. The third and fourth columns in Table I, respectively, give the basic bond and the bonding unit (minimum cluster) originating in the basic bond for *a*-SiO_x. The corresponding basic bond and bonding unit for *a*-SiN_x are shown in the fifth and sixth columns, respectively. In the RBM, the bonding structure of *a*-SiO_x or *a*-SiN_x films is given by a statistically controlled mixture of five bonding units independent of each other, occurring at $f_n(x)$ (see Table I). Indeed, on the basis of the modified RBM including hydrogen, we have shown

TABLE I. Random-bonding model for *a*-SiO_x and *a*-SiN_x. $f_n(x)$ is a generation probability. The bonding unit denotes a minimum cluster originating in the basic bonds.

| <i>n</i> | $f_n(x)$ | <i>a</i> -SiO _x | | <i>a</i> -SiN _x | |
|----------|---------------------|-------------------------------------|--------------------------------|-------------------------------------|--------------------------------|
| | | Basic bond | Bonding unit | Basic bond | Bonding unit |
| 0 | $(1 - px)^4$ | Si(Si ₄) | Si | Si(Si ₄) | Si |
| 1 | $4(px)(1 - px)^3$ | Si(Si ₃ O) | Si ₂ O | Si(Si ₃ N) | Si ₃ N |
| 2 | $6(px)^2(1 - px)^2$ | Si(Si ₂ O ₂) | SiO | Si(Si ₂ N ₂) | Si ₃ N ₂ |
| 3 | $4(px)^3(1 - px)$ | Si(SiO ₃) | Si ₂ O ₃ | Si(SiN ₃) | SiN |
| 4 | $(px)^4$ | Si(O ₄) | SiO ₂ | Si(N ₄) | Si ₃ N ₄ |

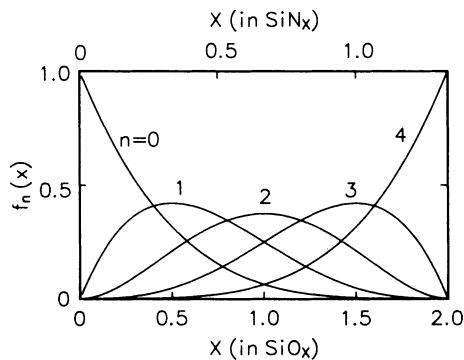


FIG. 1. Generation probability $f_n(x)$ as a function of x for SiO_x (lower axis) and SiN_x (upper axis) systems. n denotes each component of five $\text{Si}(\text{Si}_{1-n}\text{M}_n)$ ($M=\text{O}$ or N) bonding configurations.

that the density of incorporated SiH and NH bonds as a function of x in PECVD $a\text{-SiN}_x\text{:H}$ films can be explained by the x dependence of their counterparts in individual bonding units including H atoms.¹¹

C. Effective charge on atoms

If individual bonding units in the RBM (Table I) are assumed to satisfy the charge-neutrality conditions as stated in Sec. II A, the partial charge on a Si and O or N atom in each bonding unit can be evaluated using Eq. (1). The results are shown in Table II. By evaluating the statistical sum of $P_M(n)$ in Table II using $f_n(x)$ in Table I, the averaged partial charge $P_M(x)$ ($M=\text{Si}$, O, or N) on a Si, O, or N atom in $a\text{-SiO}_x$ and $a\text{-SiN}_x$ can be obtained as a function of x , as follows:

$$P_{\text{Si}}(x) = \sum_{n=0}^4 P_{\text{Si}}(n) f_n(x) / \sum_{n=0}^4 f_n(x), \quad (3)$$

and

$$P_M(x) = \sum_{n=1}^4 n P_M(n) f_n(x) / \sum_{n=1}^4 n f_n(x) \quad (M=\text{O or N}). \quad (4)$$

Here, n in Eq. (4) means the ratio of the number of O or N atoms per Si atom included in individual bonding units. As stated in Sec. II A, the effective charge on a given atom is given as $4P_M(x)$ ($M=\text{Si}$, O, or N), since f_c

of Si is 4. Figures 2(a) and 2(b) show $P_{\text{Si}}(x)$ and $P_M(x)$ ($M=\text{O}$ or N) as a function of x for $a\text{-SiO}_x$ and $a\text{-SiN}_x$, respectively. Note that the condition

$$xP_M(x) + P_{\text{Si}}(x) = 0 \quad (5)$$

is satisfied in Fig. 2 as a result of charge neutrality. Furthermore, we notice that the $P_{\text{Si}}(2)$ value ($0.40e$) at $x=2$ for $a\text{-SiO}_x$ shown in Fig. 2(a) and Table II agrees well with the result observed for crystalline SiO_2 , in which a charge transfer of $0.43e$ per single bond from Si to O atoms has been reported.²⁵

As shown in Fig. 2(a), the rate of increase of the positive charge on a Si atom with x is found to become lower with increasing x . As a result, the negative charge on an O or N atom decreases with increasing x , as shown in Fig. 2(b), although in the RBM it is assumed that the O and N atoms are bonded to Si atoms only. The decrease of this negative charge is a result of a so-called induction effect, and it is indicated that an induction effect can be analyzed in terms of the above effective-charge-analysis (ECA) model. This effect will be understood as indicating an effect of Coulomb repulsion, through a change in the effective electronegativity of individual bonding units (see Table II). Thus, the ECA model provides a convenient way for the numerical analysis of an induction effect.

III. EXPERIMENT

The samples were deposited by rf glow-discharge decomposition of a $\text{SiH}_4\text{-O}_2$ mixture in a fused-quartz reactor, employing inductive coupling of rf power, and inserted into an electric furnace set at 300°C . The details of the deposition system have been described elsewhere.²⁶ The gas volume ratios $V(\text{O}_2)/V(\text{SiH}_4)$ were varied from 0 to 1.5 under a fixed SiH_4 flow rate of 0.8 cubic centimeter per minute at STP (SCCM). The rf power was maintained at 10 W, and the pressure was 0.17 Torr. The approximately 500-Å-thick $a\text{-SiO}_x$ films were deposited onto single-crystal Si substrates. The XPS was measured by using the spectrometer (ULVAC-PHI, Model-255) with a Mg K_α radiation (1253.6 eV) source. A sample chamber was pumped down to a pressure of 1×10^{-8} Torr. The samples were cleaned just before the XPS measurements by Ar^+ ion bombardment at 3 keV, and the surface layer about 200 Å thick was stripped off. The O content x in SiO_x was determined from the integrated intensity ratio of the O 1s to Si 2p lines, using the ratio for thermally grown SiO_2 as the standard of x .

TABLE II. Partial charge, $P_{\text{Si}}(n)$, $P_{\text{O}}(n)$, and $P_{\text{N}}(n)$, on Si, O, and N atoms, respectively, in each bonding unit for $a\text{-SiO}_x$ and $a\text{-SiN}_x$. S_{Si} , S_{N} , and S_{O} are the electronegativity of Si, N, and O atoms, respectively. $S_{\text{Si}}=2.84$, $S_{\text{N}}=4.49$, and $S_{\text{O}}=5.21$.

| n | $a\text{-SiO}_x$ | | | $a\text{-SiN}_x$ | | |
|-----|-------------------------|--------------------|-------------------|-------------------------|--------------------|-------------------|
| | Bonding unit | $P_{\text{Si}}(n)$ | $P_{\text{O}}(n)$ | Bonding unit | $P_{\text{Si}}(n)$ | $P_{\text{N}}(n)$ |
| 0 | Si | 0 | | Si | 0 | |
| 1 | Si_2O | 0.182 | -0.365 | Si_3N | 0.098 | -0.296 |
| 2 | SiO | 0.287 | -0.287 | Si_3N_2 | 0.163 | -0.245 |
| 3 | Si_2O_3 | 0.356 | -0.237 | SiN | 0.209 | -0.209 |
| 4 | SiO_2 | 0.404 | -0.201 | Si_3N_4 | 0.243 | -0.182 |

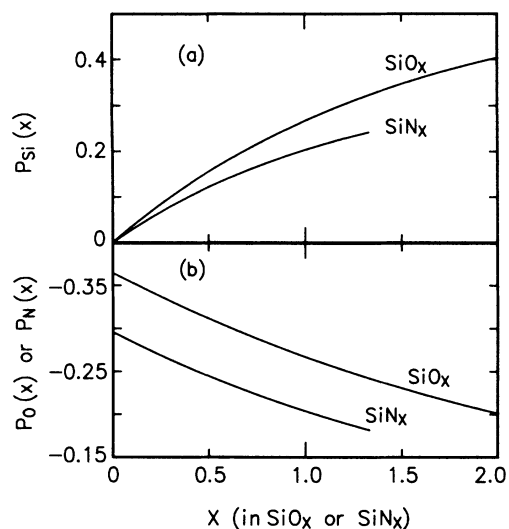


FIG. 2. (a) Averaged partial charge $P_{\text{Si}}(x)$ on a Si atom, and (b) $P_{\text{O}}(x)$ on an O atom or $P_{\text{N}}(x)$ on a N atom, as a function of x for $a\text{-SiO}_x$ and $a\text{-SiN}_x$.

IV. RESULTS AND DISCUSSION

The Si $2p$ XPS spectra from $a\text{-SiO}_x$ films exhibited an asymmetric line shape depending on x similar to those reported by Bell and Ley.¹³ In order to examine the shift of this spectrum as a function of x on the basis of the RBM, we defined the effective peak binding energies for the Si $2p$ and O $1s$ spectra, $E_B(\text{Si } 2p)$ and $E_B(\text{O } 1s)$, as a weighted average of energy with the signal height, which refers to the center of gravity of the spectrum. Figure 3 shows $E_B(\text{Si } 2p)$ and $E_B(\text{O } 1s)$ as a function of x . As stated in Sec. I, a shift of the Si $2p$ line should be due to the charge transfer from Si to more electronegative O atoms. If a change in the bonding structure of $a\text{-SiO}_x$ and $a\text{-SiN}_x$ films with varying x obeys the RBM as proposed by

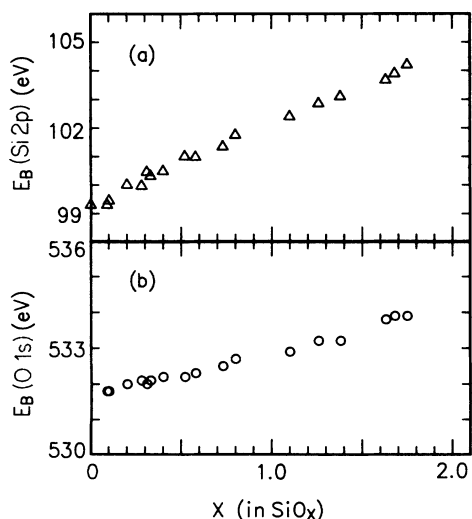


FIG. 3. (a) Effective peak binding energy $E_B(\text{Si } 2p)$ of the Si $2p$, and (b) $E_B(\text{O } 1s)$ of the O $1s$ as a function of x for $a\text{-SiO}_x$ films.

several authors,^{7,11,13,14} the shift of the Si $2p$ line shown in Fig. 3(a) can be connected with a statistical distribution of five $\text{Si}(\text{Si}_{4-n}\text{O}_n)$ ($n=0,1,\dots,4$) bonding configurations. In each configuration, the value of $E_B(\text{Si } 2p)$ increases with an increase in the n value as a result of the charge transfer stated above. Also, for the present $a\text{-SiO}_x$ films, there is evidence for the validity of the RBM. Figure 4 shows the full width at half maximum (FWHM) of the Si $2p$ spectrum as a function of x . Thus, the spectra have a maximum width at around $x=1$. Similar results have also been found for $a\text{-SiN}_x$ films, in which the Si $2p$ width has a maximum at around $x=0.7$.¹² In the RBM, as shown in Fig. 1, it is predicted that the number of components of the bonding configurations making a significant contribution to the observed XPS spectrum becomes larger at around half the stoichiometric composition. This will lead to the expected larger width. For a shift of the O $1s$ line, since the line shape was almost symmetric, the shift is expected to be due to an induction effect and/or a shift of the Fermi level as stated in Sec. I. We will defer the discussion on this shift to a later stage.

A shift of the Si $2p$ core level with an increase in x for $a\text{-SiO}_x$ or $a\text{-SiN}_x$ films should be dominated by a change of additional positive charge on the Si atoms under observation. So, if the bonding structure of these films can be described by the RBM, $E_B(\text{Si } 2p)$ is expected to be proportional to the averaged partial charge $P_{\text{Si}}(x)$ on a Si atom per single bond shown in Eq. (3) and Fig. 2(a), independent of the different kinds of sample. Figure 5 shows $E_B(\text{Si } 2p)$ as a function of $P_{\text{Si}}(x)$ for $a\text{-SiO}_x$ films in the present work along with the results for $a\text{-SiN}_x$ films in the published works.^{10,12,16} In this figure, the results for a stoichiometric SiC film,²⁷ a 25-Å-thick Si_3N_4 film,²⁸ and SiO_2 (Ref. 29) are also shown for comparison. In the case of the present films, a rather large number of H atoms are incorporated into the films. Since hydrogen has an electronegativity ($S_{\text{H}}=3.55$) larger than that of silicon ($S_{\text{Si}}=2.84$), the incorporated H atoms may affect the value of $P_{\text{Si}}(x)$. However, the value of S_{H} is considerably smaller than that of oxygen ($S_{\text{O}}=5.21$), and the H density, which had a maximum value at around $x=0.8$, was below 20 at. %. Therefore, an influence of H atoms to $P_{\text{Si}}(x)$ was found to be below around 7% at $x=0.8$ from Eq. (1).

As shown in Fig. 5, except for $a\text{-SiO}_x$ and $a\text{-SiN}_x$ films with a near-stoichiometric composition, $E_B(\text{Si } 2p)$ for all

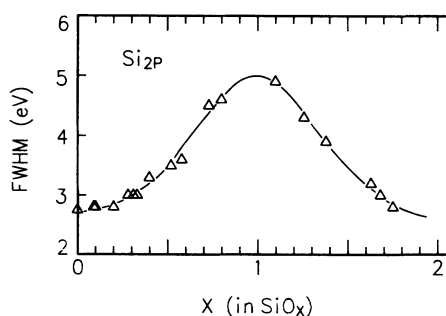


FIG. 4. FWHM of the Si $2p$ spectrum as a function of x for $a\text{-SiO}_x$ films.

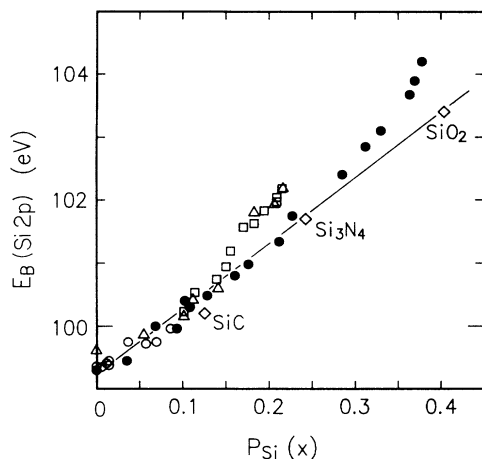


FIG. 5. Effective peak binding energy $E_B(\text{Si } 2p)$ of the Si $2p$ as a function of the averaged partial charge $P_{\text{Si}}(x)$ on a Si atom per single bond in $a\text{-SiO}_x$ films (closed circles). The results for $a\text{-SiN}_x$ films in the published works (open circles, Ref. 10; triangles, Ref. 12; squares, Ref. 16), and those for stoichiometric compounds, SiC film (Ref. 27), 25-Å-thick Si_3N_4 film (Ref. 28), and SiO_2 (Ref. 29), are shown for comparison. The solid line denotes the relation of $E_B(\text{Si } 2p) = 10.2P_{\text{Si}}(x) + 99.3$.

kinds of sample are found to fit well to an expected straight line with the relation of

$$E_B(\text{Si } 2p) = 10.2P_{\text{Si}}(x) + 99.3. \quad (6)$$

This relation will be applicable to various stoichiometric compounds and nonstoichiometric compounds, in the case where the RBM determines the bonding structure, which are composed of Si-centered tetrahedra. As stated in Sec. II C, since the additional effective charge on a Si atom is given as $4P_{\text{Si}}(x)$, Eq. (6) predicts that addition of a unit of positive charge onto a Si atom shifts $E_B(\text{Si } 2p)$ towards higher binding energy by 2.55 eV. In Fig. 5, the deviation of the data from the straight line for $a\text{-SiO}_x$ and $a\text{-SiN}_x$ films occurs at x above 1.2 and 0.7, respectively, as seen in Fig. 2(a). This deviation is probably due to a charging effect during the XPS measurement, which will be a serious problem for thicker films with a high x . As stated in Sec. III, the thickness of the present $a\text{-SiO}_x$ films were about 300 Å, and the data represented by square symbols were replotted from the results for a 500-Å-thick $a\text{-SiN}_x$ layer prepared by ion implantation.¹⁶ On the other hand, $E_B(\text{Si } 2p)$ for a 25-Å-thick $a\text{-Si}_3\text{N}_4$ film²⁸ agrees well with the value determined from Eq. (6) as shown in Fig. 5.

For $a\text{-SiO}_x$ films ($0 \leq x \leq 2$) deposited by reactive sputtering (RS), Bell and Ley¹³ have carried out careful XPS measurements by thinning the film thicknesses for eliminating a charging effect. In Fig. 6, the values of $E_B(\text{Si } 2p)$ for the RS $a\text{-SiO}_x$ films are replotted as a function of $P_{\text{Si}}(x)$ in (a) and of x in (b). As shown in Fig. 6(a), $E_B(\text{Si } 2p)$ is found to be proportional to $P_{\text{Si}}(x)$ in the entire range up to a stoichiometric composition, supporting the validity of the ECA model. On the other hand, the rate of increase of $E_B(\text{Si } 2p)$ with increasing x becomes lower in a higher x range, as shown in Fig. 6(b). As stat-

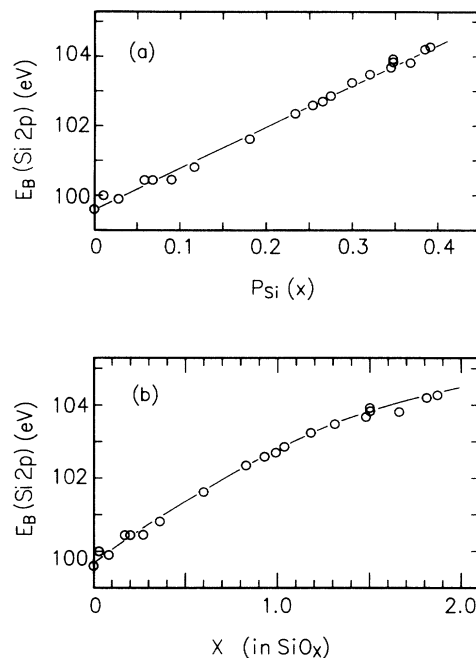


FIG. 6. Effective peak binding energy $E_B(\text{Si } 2p)$ of the Si $2p$ for RS $a\text{-SiO}_x$ films, reported in Ref. 13, as a function of (a) the averaged partial charge $P_{\text{Si}}(x)$ on a Si atom per single bond, and of (b) x .

ed in Sec. I, in the process for analyzing shifts of the Si $2p$ by means of a curve-fitting method¹²⁻¹⁴ or a weighted-average method,^{10,16} the Si $2p$ line arising from each of five $\text{Si}(\text{Si}_{4-n}\text{M}_n)$ ($M = \text{O}$ or N) bonding components has been assumed to have the same width and spacing. In this case, if the density of each component is distributed as predicted by the RBM, $E_B(\text{Si } 2p)$ is easily deduced to be proportional to x ,^{10,16} as a result of a statistical average of the peak binding energy for each component using $f_n(x)$ in Table I. This result means that $P_{\text{Si}}(x)$ is a linear function of x , since the average number of O or N atoms bonded to a Si atom is given by $2x$ or $3x$ under the RBM, respectively. This situation is tantamount to assuming the same spacing of five components as stated above. This assumption also predicts a constant value of $P_M(x)$ ($M = \text{O}$ or N) as obtained from Eq. (5), leading to fixed $E_B(\text{O } 1s)$ and $E_B(\text{N } 1s)$ values. Obviously, these predictions are inconsistent with the observed results for the Si $2p$ line shown in Fig. 6(b) and those for the O $1s$ and N $1s$ lines shown in Fig. 7, and with $P_{\text{Si}}(x)$ and $P_M(x)$ shown in Fig. 2. By contrast, the ECA model predicts that the line spacing of five components decreases with increasing n , corresponding to a change of $P_{\text{Si}}(n)$ with n shown in Table II. This leads to the expected linear relation of $E_B(\text{Si } 2p)$ to $P_{\text{Si}}(x)$ as shown in Figs. 5 and 6(a).

For a shift of the O $1s$ line with x shown in Fig. 3(b), since an O atom is bonded to two Si atoms as stated in Sec. I, an induction effect and/or a shift of the Fermi level are expected as its origins. As stated in Sec. II C, an induction effect based on the ECA model is applicable to an examination of the observed shifts. In Fig. 7(a), $E_B(\text{O } 1s)$ as a function of $P_{\text{O}}(x)$ for the present $a\text{-SiO}_x$ films is

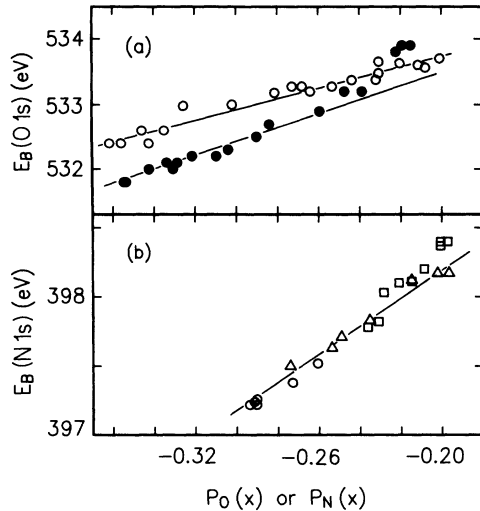


FIG. 7. (a) $E_B(\text{O } 1s)$ as a function of $P_O(x)$ for the present $a\text{-SiO}_x$ films (closed circles) and the samples (open circles) shown in Fig. 6, and (b) $E_B(\text{N } 1s)$ as a function of $P_N(x)$ for $a\text{-SiN}_x$ films shown in Fig. 5. Symbols in (b) are represented in Fig. 5.

shown along with the results for the samples in Fig. 6, and Fig. 7(b) shows $E_B(\text{N } 1s)$ as a function of $P_N(x)$ for $a\text{-SiN}_x$ films shown in Fig. 5. For sufficiently thinner RS $a\text{-SiO}_x$ films¹³ shown in Fig. 6, the $E_B(\text{O } 1s)$ values are found to be linearly related to $P_O(x)$ over the entire range, as shown by open-circle symbols in Fig. 7(a), as well as the result for $E_B(\text{Si } 2p)$ as a function of $P_{\text{Si}}(x)$ shown in Fig. 6(a). The values of $E_B(\text{O } 1s)$ for the present $a\text{-SiO}_x$ films in Fig. 7(a) and of $E_B(\text{N } 1s)$ for $a\text{-SiN}_x$ films in Fig. 7(b) can also be linearly combined with $P_O(x)$ and $P_N(x)$, respectively, except for the data in a higher range of $P_O(x)$ or $P_N(x)$, which corresponds to a higher x range. The deviation of $E_B(\text{O } 1s)$ and $E_B(\text{N } 1s)$ from the linear relation for these samples is found to correspond with the results for $E_B(\text{Si } 2p)$ shown in Fig. 5. Therefore, this deviation will be attributed to a charging effect during the XPS measurements as stated above.

As stated in Sec. II A, the effective negative charge on an O and a N atom is given by $4P_O(x)$ and $4P_N(x)$, respectively. Therefore, from Figs. 7(a) and 7(b), we find that subtraction of a unit of negative charge from an O and N atom, respectively, shifts the O 1s core level by 1.0–1.4 eV and the N 1s core level by about 1.3 eV toward higher binding energy. Thus, a range of the shifts per unit charge in both O 1s and N 1s core levels are found to be almost the same energy of 1.2 ± 0.2 eV, which is about half of that for the Si 2p core level (2.55 eV) as stated above (see Fig. 5). Such a similar behavior between the shifts in the O 1s and N 1s arises because both core levels lie at similar deeper levels below the Fermi level, that is, around 530 eV for the former and around 400 eV for the latter. By contrast, the core level for the Si 2p is around 100 eV. Thus, the downward shifts of both $E_B(\text{O } 1s)$ and $E_B(\text{N } 1s)$ with increasing x can be explained by a decrease in the effective negative charge on a

N and an O atom due to an induction effect based on the ECA model. In contrast to the present model, Kärcher, Ley, and Johnson¹² and Bell and Ley¹³ have proposed that the shifts of $E_B(\text{N } 1s)$ and $E_B(\text{O } 1s)$ are caused mainly by upward shifts of the Fermi level in $a\text{-SiN}_x$ and $a\text{-SiO}_x$ films with increasing x (see Sec. I).

V. SUMMARY

For PECVD $a\text{-SiO}_x$ films deposited at 300°C using $\text{SiH}_4\text{-O}_2$ mixtures, the shifts of XPS spectra from the Si 2p and O 1s core levels were investigated as a function of the O content x . The effective Si 2p and O 1s binding energies $E_B(\text{Si } 2p)$ and $E_B(\text{O } 1s)$, defined as the peak energy at the center of gravity of the spectrum, shifted toward higher binding energy. In order to examine these shifts, we have considered an ECA model, in which the averaged partial charge $P_M(x)$ ($M = \text{Si}$ or O) on a Si and an O atom was evaluated as a function of x by using the Sanderson's calculational method of partial charge on atoms,²⁴ on the basis of the RBM. This ECA model was applied to the XPS results for the present $a\text{-SiO}_x$ films, and to other published results for $a\text{-SiO}_x$, $a\text{-SiN}_x$, and SiC samples. As a result, the observed $E_B(\text{Si } 2p)$ for all kinds of sample was found to be linearly related to $P_{\text{Si}}(x)$,

$$E_B(\text{Si } 2p) = 10.2P_{\text{Si}}(x) + 99.3.$$

Since $P_{\text{Si}}(x)$ means the effective ionicity of the Si per single bond, the additional effective charge on a Si atom is given as $4P_{\text{Si}}(x)$. Therefore, the above equation predicts that addition of a unit of positive charge onto a Si atom shifts $E_B(\text{Si } 2p)$ towards higher binding energy by 2.55 eV. Furthermore, the present ECA model showed that spacing of the Si 2p line arising from each of five $\text{Si}(\text{Si}_{4-n}\text{M}_n)$ ($n = 0, 1, \dots, 4; M = \text{O}$ or N) bonding units based on the RBM decreases with increasing n , although this spacing has been taken to be the same in the analysis of XPS by many workers.^{10, 12–14, 16}

The evaluated negative partial charge, $P_O(x)$ or $P_N(x)$, on an O or N atom decreased with increasing x , although almost all O and N atoms in $a\text{-SiO}_x$ and $a\text{-SiN}_x$ are bonded to Si atoms only. This is understood as a so-called induction effect. The observed $E_B(\text{O } 1s)$ and $E_B(\text{N } 1s)$ values were shown to be linearly related to $P_O(x)$ and $P_N(x)$, respectively. From these linear functions, as a unit of negative charge is subtracted from an O and a N atom, both $E_B(\text{O } 1s)$ and $E_B(\text{N } 1s)$ were found to shift by almost the same energy of 1.2 ± 0.2 eV toward higher binding energy. Thus, the ECA model is seen to provide a convenient way of numerical analysis of the shifts in XPS spectra for various samples, if their bonding structure obeys the RBM. Furthermore, it may also permit application to an analysis of shifts in vibrational spectra.

ACKNOWLEDGMENTS

The authors are indebted to S. Ueda for use of the XPS spectrometer, and also to T. Nakazawa for his help with the measurements.

- ¹M. J. Powell, B. C. Easton, and O. F. Hill, *Appl. Phys. Lett.* **38**, 794 (1981).
- ²K. Ghandi, *VLSI Fabrication Principles* (Wiley-Interscience, New York, 1983), p. 427.
- ³F. J. Grunthaler and P. J. Grunthaler, *Mater. Sci. Rep.* **1**, 65 (1986).
- ⁴J. J. Chang, *Proc. IEEE* **64**, 1039 (1976).
- ⁵A. K. Sinha, H. J. Levinstein, T. E. Smith, G. Quintana, and S. E. Haszko, *J. Electrochem. Soc.* **125**, 601 (1978).
- ⁶B. Abeles and T. Tiedje, *Phys. Rev. Lett.* **51**, 2003 (1983).
- ⁷W. R. Knolle and J. W. Osenbach, *J. Appl. Phys.* **58**, 1248 (1985).
- ⁸A. J. Lowe, M. J. Powell, and S. R. Elliott, *J. Appl. Phys.* **59**, 1251 (1986).
- ⁹A. Morimoto, H. Niriya, and T. Shimizu, *Jpn. J. Appl. Phys.* **26**, 22 (1987).
- ¹⁰S. Hasegawa, T. Tsukao, and P. C. Zalm, *J. Appl. Phys.* **61**, 2916 (1987).
- ¹¹S. Hasegawa, M. Matsuda, and Y. Kurata, *Appl. Phys. Lett.* **57**, 2211 (1990); *ibid.* **58**, 741 (1991).
- ¹²R. Kärcher, L. Ley, and R. L. Johnson, *Phys. Rev. B* **30**, 1896 (1984).
- ¹³F. G. Bell and L. Ley, *Phys. Rev. B* **37**, 8383 (1988).
- ¹⁴G. M. Ingo, N. Zacchetti, D. della Sala, and C. Coluzza, *J. Vac. Sci. Technol. A* **7**, 3048 (1989).
- ¹⁵R. Hezel and N. Lieske, *J. Electrochem. Soc.* **129**, 379 (1982).
- ¹⁶S. Hasegawa and P. C. Zalm, *J. Appl. Phys.* **58**, 2539 (1985).
- ¹⁷G. Lucovsky, *Solid State Commun.* **29**, 571 (1979).
- ¹⁸G. Lucovsky, J. Yang, S. S. Chao, J. E. Tyler, and W. Czuba-tyj, *Phys. Rev. B* **28**, 3225 (1983); *ibid.* **28**, 3234 (1983).
- ¹⁹D. L. Griscom, *J. Non-Cryst. Solids* **24**, 155 (1977).
- ²⁰E. Parthe, *Crystal Chemistry of Tetrahedral Structure* (Gordon and Breach, New York, 1964), p. 73.
- ²¹Y. Katayama, K. Usami, and T. Shimada, *Philos. Mag. B* **43**, 283 (1981).
- ²²L. Pauling, *The Nature of Chemical Bonds*, 3rd ed. (Cornell University Press, New York, 1960), p. 85.
- ²³R. T. Sanderson., *Chemical Periodicity* (Reinhold, New York, 1960), pp. 16–56.
- ²⁴R. T. Sanderson, *Chemical Bonds and Bond Energy*, 2nd ed. (Academic, New York, 1976), p. 77.
- ²⁵J. Chelikowsky and M. Schluter, *Phys. Rev. B* **15**, 4020 (1977).
- ²⁶S. Hasegawa, S. Narikawa, and Y. Kurata, *Philos. Mag. B* **48**, 431 (1983).
- ²⁷T. Takeshita, Y. Kurata, and S. Hasegawa, *J. Appl. Phys.* **71**, 5395 (1992).
- ²⁸A. Iqbal, W. B. Jackson, C. C. Tsai, J. W. Allen, and C. W. Bates, *J. Appl. Phys.* **61**, 2947 (1987).
- ²⁹C. D. Wagner, W. M. Riggs, L. E. Davis, and J. F. Moulder, *Handbook of X-ray Photoelectron Spectroscopy*, edited by G. E. Muilenberg (Perkin-Elmer, Minnesota, 1978), p. 52.